European Journal of Pharmaceutical Sciences 214 (2025) 107283

Contents lists available at ScienceDirect

European Journal of Pharmaceutical Sciences

journal homepage: www.elsevier.com/locate/ejps

Approaching drug release performance from mesoporous silica formulations by modeling of chemical potentials

Andreas Niederquell [a,b], Annika Hofer [b], Barbora Vraníková [a], Martin Kuentz [b,*]

[a] Department of Pharmaceutical Technology, Faculty of Pharmacy in Hradec Králové, Charles University, Akademika Heyrovského 1203, 500 05 Hradec Králové, Czech Republic

[b] Institute for Pharma Technology, University of Applied Sciences and Arts Northwestern Switzerland, School of Life Sciences FHNW, Hofackerstr. 30, 4132 Muttenz, Switzerland

ARTICLE INFO

Keywords:
Drug dissolution
Chemical potentials
Silica-water partitioning coefficient
Non-ordered mesoporous silica
COSMO-RS
Drug-silica interactions

ABSTRACT

Mesoporous silica are promising bio-enabling carriers for poorly soluble drugs. However, a comprehensive understanding of drug-silica interactions and their impact on drug release remains limited. Apart from urgently needed experimental tools, predictive *in silico* tools that consider drug-carrier interactions in aqueous media are currently lacking. To address this gap, a novel *in silico* approach (silica-water partitioning coefficient) was introduced in this study. A series of ten drugs were loaded onto a mesoporous carrier (Parteck® SLC 500), and the products were analyzed using differential scanning calorimetry (DSC) and X-ray powder diffraction (XRPD). In vitro dissolution (USP II) profiles of drug-loaded formulations were analyzed and correlated with a newly introduced silica-water partitioning coefficient derived from chemical potential calculations using the Conductor-like Screening Model for Real Solvents (COSMO-RS). Strong correlations were observed between dissolution parameters, such as the initial release slopes (Pearson r = -0.98; $p = < 0.05$) and AUC values (Pearson r = -0.79; $p < 0.05$), and the calculated chemical potential-based partitioning coefficient. This study introduces a predictive method based on COSMO-RS-derived chemical potentials to estimate silica-water partitioning for drugs, thereby predicting their release performance from mesoporous silica formulations. The results demonstrate that these calculated chemical potentials can qualitatively rank the drug release kinetics in aqueous media. Further investigation with additional compounds and carrier types may broaden the applicability of this approach as a mechanistic tool for mesoporous silica formulation development and contribute to narrowing the gap toward future clinical translation.

1. Introduction

Mesoporous silica-based formulations (MS) and amorphous solid dispersions (ASDs) are well-established formulation strategies to enhance the solubility and stability of poorly water-soluble drugs by stabilizing the drug in a non-crystalline form (Argyo et al., 2014; Bremmell and Prestidge, 2019; Kawabata et al., 2011; Khan et al., 2022; Maleki et al., 2017; McCarthy et al., 2016; Mehmood et al., 2017; Narayan et al., 2018; Prestidge et al., 2007; Qian and Bogner, 2012; Roggers et al., 2014; Santos et al., 2011; Tang et al., 2012; Vallet-Regí et al., 2018). ASDs typically consist of a drug molecularly dispersed in a polymer matrix that stabilizes the amorphous form by increasing the glass transition temperature and reducing molecular mobility. Supersaturation upon dissolution is often maintained through polymer-drug interactions and the inhibition of nucleation and crystal growth (Chiou and Keyphrases, 1971; Leuner and Dressman, 2000). In contrast to polymer-based amorphous solid dispersions, mesoporous silica (MS) formulations utilize inorganic carriers with defined mesopores to confine drug molecules in a spatially restricted environment. According to the IUPAC classification, mesoporous materials possess pore diameters between 2 and 50 nm, a range particularly relevant for drug delivery, as it enables efficient adsorption while permitting molecular mobility for desorption. This physical confinement, in combination with interfacial interactions at the silica surface, can suppress crystallization and modulate drug release kinetics. Although such systems often have limited drug-loading capacity and typically do not

* Corresponding author at: University of Applied Sciences and Arts Northwestern Switzerland, Pharma Technology and Biotechnology, Hofackerstr. 30, CH-4132 Muttenz Switzerland.
E-mail address: martin.kuentz@fhnw.ch (M. Kuentz).

https://doi.org/10.1016/j.ejps.2025.107283
Received 15 July 2025; Received in revised form 10 September 2025; Accepted 18 September 2025
Available online 19 September 2025
0928-0987/© 2025 The Authors. Published by Elsevier B.V. This is an open access article under the CC BY license (http://creativecommons.org/licenses/by/4.0/).

inherently maintain supersaturation in aqueous media, they can offer advantages over conventional ASD approaches based on hot-melt extrusion or spray drying. These advantages may include improved physical stability through spatial confinement, as well as enhanced chemical stability (Ditzinger et al., 2019; Zhang et al., 2022). The material used in this study, Parteck® SLC 500, is a disordered mesoporous silica with a high specific surface area and an average pore diameter within the mesoporous range (6.1 ± 0.01 nm) (Vraníková et al., 2020). It has been previously applied in studies on drug-silica interactions and loading-dependent amorphous stability (Niederquell et al., 2023; Vraníková et al., 2020). Beyond their stabilizing capacity, MS materials are pharmaceutically attractive due to their GRAS (Generally Recognized as Safe) status and ability to shield drugs from moisture, oxygen, and light.

In the literature, MS have frequently been discussed in the context of stabilizing poor glass formers i.e., compounds with low glass-forming ability (GFA class I and II) that are prone to recrystallization and often require precipitation inhibitors for supersaturation maintenance (Baird et al., 2010; Wyttenbach et al., 2016). However, MS drug delivery is equally relevant for GFA class III compounds, which are intrinsically more stable in their amorphous form and tend to remain metastable in supersaturated solutions, often without requiring polymeric precipitation inhibitors. Although MS-based formulations have yet to gain widespread adoption in the pharmaceutical market, their unique capabilities in stabilizing and delivering poorly soluble drugs are driving ongoing research and development efforts, making them a versatile drug delivery platform. However, a significant knowledge gap remains regarding the molecular interactions between individual drugs and silica surfaces and how these interactions influence stability and drug release. Besides this research gap, most publications focus on only one to three model compounds, even though it is important to study a broader dataset. Additionally, the performance of MS formulations is often benchmarked against crystalline drug forms using dissolution experiments, which are time-consuming. Therefore, it would be beneficial to have either computational or simple experimental tools to anticipate release performance before embarking on time-consuming biopharmaceutical in vitro experimentation. To approach these research gaps, our recent investigations explore intrinsic and apparent molecular interactions between drugs and mesoporous silica, particularly concerning formulation stability (Niederquell et al., 2025, 2023). While intrinsic affinity represents a direct binary interaction between the drug and silica surface, an apparent interaction occurs in the presence of a solvent or water phase.

An important experimental methodology in this context has been the use of so-called in situ sorption studies, as demonstrated by the group of Lynne Tailor, which provide valuable insight into drug adsorption onto mesoporous silica surfaces (Dening et al., 2019; McCarthy et al., 2020). The drug loading sorption method involves the adsorption of drug molecules from a solution onto mesoporous silica materials based on interactions between the drug and the silica surface. When the drug is in a supersaturated solution, it can adsorb onto the large surface area of silica, forming both monolayers and multilayers within the mesopores. The driving forces for this sorption include hydrogen bonding between the drug and surface silanol groups of the silica, and other interaction mechanisms like electrostatic forces and Van der Waals forces (Eugene Papirer, 2000; Hate et al., 2020a; Niederquell et al., 2025).

Apart from experimental studies of drug-carrier interactions, much work has been done also in silico, but most approaches focused on the binary interaction of drug and silica (Delle Piane et al., 2014; Gignone et al., 2015; Narayan et al., 2022; Niederquell et al., 2023). Accordingly, these molecular modeling approaches calculate the intrinsic interactions between the drug and the mesoporous silica carrier, which may be useful for drug loading or stability considerations. However, their relevance to drug release remains unclear because water has not been explicitly considered. Water has been otherwise considered in, for example, other predictions based on the conductor-like screening model (COSMO), which has been used in the pharmaceutical field, ranging from solubility predictions (Klajmon, 2022; Klamt et al., 2002; Mac Fhionnlaoich et al., 2024) to partitioning analyses (Mahmoudabadi and Pazuki, 2020; Warnau et al., 2021). These prior applications highlight the ability of the model for so-called “real solvents”, i.e., COSMO-RS, to capture solvation and partitioning phenomena that have pharmaceutical relevance. Therefore, it would be interesting to use such modeling also in the context of drug-silica interactions in an aqueous environment.

A particular strength of COSMO-RS is the combination of quantum-chemical surface charge predictions with thermodynamic modeling (Loschen and Klamt, 2015). By calculating the chemical potentials of the drug in a silica or water environment, a silica-water partitioning coefficient can be obtained. We tested whether a COSMO-RS-derived silica-water partition coefficient could be compared and correlated with dissolution kinetics of ten mesoporous silica formulations. Rather than aiming to optimize formulation parameters such as supersaturation or physical stability, the focus was on assessing whether the calculated affinities toward silica and water can explain the extent and rate of drug desorption into aqueous media. To this end, drug loading was restricted to the theoretical monolayer adsorption capacity, thereby minimizing potential interference from crystallization or intermolecular drug-drug interactions. In addition, primarily glass-forming ability (GFA) class III compounds were selected for their good amorphous stability, reducing the likelihood of drug crystallization either during loading or on drug release, which would both be a perturbing factor in the framework of the current study to compare the silica partition coefficient with experimental release performance. As the latter quality attributes of drug release, the logarithmic initial slope of drug release rate and the logarithmic area under the concentration-time curve (AUC) were considered. Beyond identifying correlations, this study also sought to provide mechanistic insights into drug release behavior from mesoporous carriers, supporting early preformulation with the assessment of such a formulation strategy and later guiding the rational development of silica-based drug products.

2. Materials and methods

2.1. Materials

The model drugs (Fig. 1), including carvedilol, diclofenac (free acid), ivermectin, ketoconazole, lopinavir, pimozide, probucol, and ritonavir, were obtained from Biosynth Ltd. (Compton, United Kingdom), and indomethacin was purchased from Acros Organics Ltd. (Geel, Belgium), and quinidine was received from Sigma-Aldrich Chemie Ltd. (Buchs, Switzerland). The disordered mesoporous silica carrier Parteck® SLC 500 was kindly supplied by Merck KGaA (Darmstadt, Germany). Organic solvents such as acetone, acetonitrile, dichloromethane, and methanol, as well as other chemicals such as potassium dihydrogen phosphate, sodium hydroxide, and dioctyl sulfosuccinate sodium salt (DOSS), were obtained from Merck KGaA. Ammonium acetate and acetic acid were purchased from Fluka Analytical - Honeywell Inc. (Charlotte, USA). Ortho-phosphoric acid was procured from Carl Roth GmbH & Co. KG (Karlsruhe, Germany). The water used throughout the study was prepared with an Arium® 61,215 water purification system from Sartorius Stedim Biotech Ltd. (Göttingen, Germany). All excipients were used as supplied, without further purification.

2.2. Methods

2.2.1. Drug state characterization

2.2.1.1. Differential scanning calorimetry (DSC). Differential scanning calorimetry was used to characterize the physical state of the drug substances. The measurements were carried out with the STARe System DSC 3 from Mettler Toledo GmbH (Greifensee, Switzerland). The heat

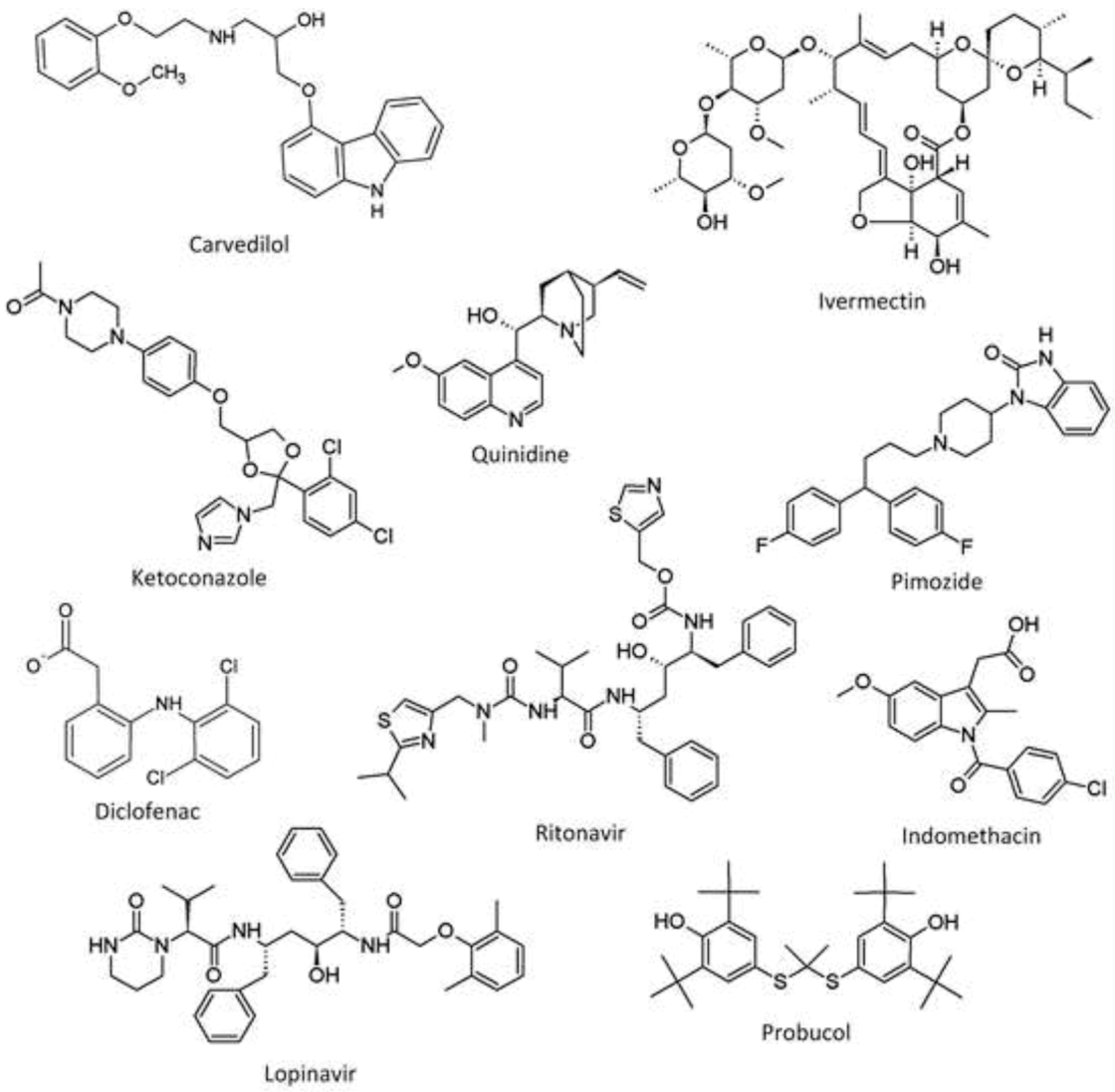

Fig. 1. 2D chemical structures of 10 selected pharmaceutical active substances.

flow difference between the two independent furnaces was measured, with the blank furnace used as a reference. The pure active ingredients, blank mesoporous silica carrier, and drug-loaded silica powders were measured. In addition, physical mixtures consisting of silica particles and active ingredients were analyzed at a ratio corresponding to the monolayer loading capacity (MLC). For this purpose, 5 to 10 mg of the sample was placed and crimped in a standard 40 µL aluminum pan with pierced lids. The samples were subjected to two heating and two cooling cycles. The temperature was varied from 25 to 270 °C with a heating/cooling rate of 10 °C/min. The data were analyzed using the STARe software.

The glass forming ability (GFA) of the drug substances was classified based on their crystallization behavior during thermal processing using the same DSC measurement method. A more detailed description of the method can be found in the literature (Baird et al., 2010). Compounds were categorized into three GFA classes according to established criteria:

GFA Class I (poor glass formers): These compounds crystallize readily upon cooling from the melt, indicating a low resistance to recrystallization and poor glass stability.

GFA Class II (intermediate glass formers): These substances form an amorphous glass upon cooling but tend to recrystallize either during storage or upon subsequent reheating, suggesting moderate kinetic resistance to crystallization.

GFA Class III (good glass formers): These compounds remain amorphous upon both cooling and reheating, demonstrating high glass stability and a minimal crystallization tendency from the melt.

2.2.1.2. X-ray powder diffraction (XRPD). In addition to the measurements of pure drugs, X-ray diffractograms were recorded to confirm the amorphous character and evaluate the stability of the physical mixtures and drug-loaded mesoporous silica formulations. Therefore, an X-ray diffractometer (R-XRD Phaser D2) from Bruker AXS Ltd. (Karlsruhe, Germany) was employed. The device was equipped with a Co and Cu KFL tube (30 kV, 10 mA) as the radiation source and a 1-D Lynxeye® detector. The measurements were carried out at a voltage of 30 kV and a current of 10 mA. The sample was rotated at 15 rpm, and the anguar scanning range for each sample was from 6° (2θ) to 40° (2θ) with a step size of 0.02° (2θ) at 2.0 s per step. Under these conditions, the detection limit for the crystalline content was approximately 1 % w/w.

2.2.2. Loading of the mesoporous silica particles

The monolayer capacity (MLC), which is the drug loading for a theoretical monolayer adsorption on mesoporous silica surfaces, was calculated using Eq. (1). This approach has been well described in the

literature (Bavnhøj et al., 2019; Dening and Taylor, 2018; Le et al., 2019). The specific surface area (SSA) for the utilized silica particles was taken from previously published measurements (Niederquell et al., 2023) using nitrogen and the "Brunauer Emmett Teller" (BET) method. N_A represents Avogadro's number, M_w is the molecular weight, and for the maximum projected contact area (SA_M), the two largest molecular dimensions of the individual drug molecules were used, which were estimated using the Molecular Modeling Pro Plus 8.2.1 software (Norgwyn Montgomery Software Inc., North Wales, USA).

$$MLC\ [\%,\ g/g] = \frac{SSA \cdot M_w \cdot 10^{20}}{SA_M \cdot N_A} \quad (1)$$

The drug-loading of the mesoporous silica powder (Parteck® SLC 500) was carried out according to the incipient wetness impregnation method (Khalbas et al., 2024a, 2024b). For the loading process, a Chemyx Fusion 200 syringe pump from Chemyx Inc. (Stafford, USA) was employed. Before loading, the silica particles were dried for 12 h at 100 °C and a vacuum of 550 mbar in a vacuum drying oven of type KVST-11 from Salvis Plc. (Reussbühl, Switzerland). Two different solvents were used for loading due to the different solubilities of the active ingredients. Acetone was used for carvedilol, diclofenac (free acid), and lopinavir, while dichloromethane was the choice for indomethacin, ivermectin, ketoconazole, pimozide, probucol, quinidine, and ritonavir. All drug solutions had a concentration of 20 mg/mL and were added dropwise to 1 g of mesoporous silica at a rate of 0.1 mL/min while using continuous mild stirring (50 rpm) of the mesoporous silica (MS) carrier on a magnetic stirring plate. Using a precise automated syringe pump for the dropwise drug loading, a typical accuracy of about ± 2 % can be achieved. Subsequently, the samples were placed in a drying cabinet to allow solvent evaporation. Taking the calculated MLC into account (see Table 1), the MS carrier was loaded with different volumes of drug solution. The loaded silica samples were then left for 24 h at 60 °C and a vacuum of 500 mbar in a KVTS-11 drying oven. This temperature was chosen due to the boiling points of the solvents: acetone ~ 56 °C and dichloromethane ~ 40 °C. The loaded mesoporous silica samples were then sealed airtight and stored in a desiccator to protect them from moisture until further use. The actual gained mass after drug-loading and drying was verified gravimetrically and kept as close as possible to the calculated MLC. Therefore, the silica particles were weighed on the XS205DU analytical balance from Mettler Toledo GmbH (Greifensee, Switzerland) with a readability of 0.01 mg. The mass gain in percent (% g/g) was determined based on the weight difference between the dried empty silica carrier and that after drug loading and drying.

2.2.3. Solubility determination

Samples ($n = 3$) were prepared by adding excess drug to 4 mL of dissolution medium (phosphate buffer at pH 6.8 with 0.5 % (w/v) dioctyl sulfosuccinate sodium salt (DOSS)). The samples were left at room temperature (25 °C) for 24 h with continuous stirring on a magnetic stirrer at 200 rpm. Subsequently, to separate undissolved drug particles, the samples were centrifuged at 15,000 rpm for 10 min in an Eppendorf 5420 microcentrifuge from Eppendorf Plc. (Hamburg, Germany) and additionally filtered with titanium HPLC syringe filters (diameter: 17 mm, membrane: PTFE, pore size: 0.45 µm). The samples were diluted with dissolution medium, and the concentrations were determined using HPLC.

Table 1
Calculated theoretical Monolayer Capacity (MLC), mobile phase composition, and UV wavelength for the HPLC concentration determination of 10 individual drugs. Eluents A and Bx are specified in the text.

Substance name	MLC [% g/g]	Mobile phase composition eluent A [% v/v] and given Bx [% v/v]		Wavelength [nm]
Carvedilol	16.1	60	40 (B2)	240
Diclofenac (free acid)	22.1	70	30 (B3)	270
Indomethacin	18.6	70	30 (B3)	260
Ivermectin	22.3	95	5 (B1)	245
Ketoconazole	12.4	70	30 (B3)	244
Lopinavir	19.3	70	30 (B1)	215
Pimozide	19.5	70	30 (B3)	280
Probucol	22.6	98	2 (B1)	242
Quinidine	21.2	70	30 (B3)	235
Ritonavir	19.9	70	30 (B3)	215

2.2.4. Dissolution measurements

For the release of the loaded silica formulations, a USP type II (model DT 600) dissolution apparatus from ERWEKA, Plc. (Langen, Germany) was used. A phosphate buffer at pH 6.80 ± 0.02 with 0.5 % (w/v) DOSS was used as the release medium. The pH was adjusted to 6.8 with 1 M sodium hydroxide solution before adding 0.5 % (w/v) DOSS. This surfactant concentration was selected to ensure sufficient wetting and dispersion of the mesoporous silica while avoiding notable micellar solubilization, which could obscure drug-silica interaction effects. The paddle position was adjusted to 25 ± 2 mm above the vessel bottom in accordance with USP requirements. Each vessel contained 250 mL of release medium, and the paddle speed was set at 25 rpm. In each vessel, 120 mg of the drug-loaded mesoporous silica formulation was introduced, where the drug amount targeted the MLC of the given drug. At intervals of 2, 3, 4, 5, 10, 15, 20, 30, 40, 50, 60, 75, 90, 120, 150, and 180 min, 2 mL each were sampled and replaced with the same volume of fresh phosphate buffer. The collected samples were filtered using an HPLC titanium syringe filter (diameter: 17 mm and 0.45 µm pore size of the PTFE membrane) into HPLC vials. The concentration of the samples was then analyzed via HPLC in triplicates.

2.2.5. Concentration determination using high-performance liquid chromatography (HPLC)

The HPLC measurements were performed on an Agilent Infinity 1260 II system (Agilent Technologies GmbH, Waldbronn, Germany), which was equipped with the following components: G7167A multisampler, G7112B binary pump, G1316A column oven (Agilent 1100 series), and G1314B variable wavelength detector (Agilent 1200 series). The column used was an XBridge BEH C18 from Waters Ltd. (Eschborn, Germany) with a pore size of 130 Å, particle size of 5 µm, inner diameter of 4.6 mm, and length of 150 mm. Data acquisition and evaluation were done with the Agilent OpenLab CDS ChemStation software Rev. C.01.10 [287].

Various mobile phases were used for HPLC analysis. Acetonitrile was used in combination with either purified water (B1), purified water with 0.1 % phosphoric acid (v/v) at a pH of 2.3 (B2), or purified water with 0.1 % acetic acid (v/v) and 10 mM ammonium acetate at a pH value of 4.5 (B3). Prior to use, the mobile phases were additionally filtered through a polyethersulfone (PES) membrane filter (pore size: 0.22 µm, diameter: 47 mm) from Membrane Solutions, LLC. (Auburn, USA) at a vacuum of 300 mbar. Calibration curves were made by preparing stock solutions with 1 mg/mL of the individual drugs in acetonitrile. The stock solutions were filtered through 17 mm-sized titanium HPLC syringe filters (membrane: PTFE, pore size: 0.45 µm) from Infochroma Plc. (Goldau, Switzerland). The theoretical monolayer capacity (MLC) was considered, and the stock solutions were further diluted to 1:2, 1:4, 1:8, 1:16, 1:32, 1:64, and 1:100 (v/v). Each dilution was prepared and measured in triplicates. The measurement methods were optimized based on pre-experimental runs, and for the concentration determinations for each API, individual settings, such as mobile phase compositions and wavelengths, were chosen (see Table 1). The measurements were performed at 25 °C, an injection volume of 10 µL, and a flow rate of 0.8 mL/min, except for lopinavir, where a flow rate of 0.6 mL/min was used, were employed.

2.2.6. Molecular modeling - calculation of chemical (pseudo-) potentials

Chemical potentials of drug in a silica phase ($\mu s_{(silica)}$) or aqueous environment ($\mu s_{(water)}$) and the chemical potential for self-association of

drug molecules ($\mu s_{(self)}$) were calculated using COSMOquick v. 2020 from BIOVIA, Dassault systems SE (Vélizy-Villacoublay Cedex, France). 10 drugs were assigned as solutes, whereas a water molecule and a small slab of amorphous silica were used as the molecular basis for modeling of the phases for drug partitioning. Fig. 2 depicts a schematic representation of the entire COSMO-RS workflow for obtaining chemical (pseudo-) potentials. In brief, COSMO-RS is based on Density Functional Theory (DFT) calculations to generate a discrete molecular surface embedded in a virtual conductor (Klamt, 2011). Each segment of this surface is characterized by its area and shielding charge density (σ), which reflects the electrostatic screening by the environment and the back-polarization of the solute molecule. The resulting surface charge density distribution is then adapted to the actual dielectric constant of the solvent, effectively simulating the electrostatic interactions between the molecule and the solvent (Eckert and Klamt, 2002). While the surface charge density distribution is obtained by DFT calculations, subsequent statistical thermodynamics of these surface segments are used to determine the chemical potentials (μ) of molecules in liquids (Klamt, 2005; Klamt et al., 1998). Compared to the general COSMO-RS scheme, the COSMOquick approach applied in this work offered accelerated computation by assembling sigma profiles of new molecules from a large database of DFT results using a fragment-based method, as previously described in the literature (Loschen and Klamt, 2012).

In line with the workflow (Fig. 2), diverse equilibrium properties and complete phase diagrams can be calculated. (Eckert and Klamt, 2002; Klamt et al., 1998). The present study was making use of the calculated (pseudo-) potentials to obtain a drug to silica affinity parameter in presence of water, which can be viewed as a partitioning coefficient between a solute and the carrier surface and water. In general, solute equilibration between any two phases, P1 and P2, provides a partition coefficient $K_{(P1\text{-}P2)}$ according to Eq. (2):

$$K_{(P1-P2)} = exp\left(\frac{\mu^0{}_{P2} - \mu^0{}_{P1}}{RT}\right) \quad (2)$$

where μ^0 is the chemical potential under standard conditions (with the phase as a subscript), R is the gas constant, and T is the temperature. In the present study, drug partitioning between a silica surface and an aqueous bulk phase was of interest. For practical purposes, the thermodynamic calculations may assume the silica surface as a supercooled bulk phase, and for the chemical potentials, μ_s denotes a given chemical (pseudo-) potential that was obtained by the described COSMOquick approach. Subsequently, a silica-water partition coefficient $K_{si\text{-}w}$ was estimated using Eq. (3):

$$\ln(K_{Si-W}) \cong \left(\frac{\mu_{S(water)} - \mu_{S(silica)}}{RT}\right) \quad (3)$$

2.2.7. Statistical analysis and data representation

Correlation analyses were performed using Statgraphics Centurion v. 19.6.06 (Statgraphics Technologies Inc., Warrenton, USA). Correlation analyses were based on the calculated chemical potentials and drug dissolution performance parameters, including the initial slope and AUC values. Linear Pearson correlation coefficients were calculated and complemented with Spearman rank correlations regarding the possible occurrence of nonlinearity or outliers. The initial dissolution slope was obtained from the linear range (interpolation of the first few concentration points) of the release curves. For the representation of graphs and calculation of AUC-values ("quick tool for integration") for each drug from the whole dissolution curves ($n = 3$), the software OriginPro 2017 from OriginLab Corp. (Northampton, USA) was used. Other calculations were based on Excel from the 365 apps for enterprise package from Microsoft Corp. (Redmond, USA). The standard deviations were generally obtained from experiments in triplicate unless stated otherwise.

3. Results and discussion

3.1. Manufacture and physical analysis of formulations

In the early stages of preformulation, it is necessary to assess the potential of any formulation technology for new drug candidates. Therefore, an *in silico* ranking of drug dissolution from mesoporous silica products would be highly valuable for pharmaceutical scientists. Currently, there are some molecular simulations, but in a full-atomistic version, they can only treat comparatively small systems, especially when a quantum-chemical approach has been taken (Delle Piane et al., 2014; Gignone et al., 2015). Moreover, the currently available simulations in pharmaceutics focus on binary drug-silica interactions without considering an aqueous phase for drug release. COSMO-RS is interesting in this context as it combines quantum-chemical calculations with statistical thermodynamics of the surface segments (Klamt, 2005, 1995; Klamt et al., 1998). The present work focused on the difference in the calculated chemical potentials normalized by RT, and in line with Eq. (3), this is a drug's silica to water partition coefficient. Although the solid silica is hereby treated as a supercooled liquid, which is a simplified approximation, this approach provides a practical way to calculate chemical potentials. Accordingly, these values should be deemed as first approximations that can be suitable for ranking of compounds regarding experimental drug release performance. This consideration provided a

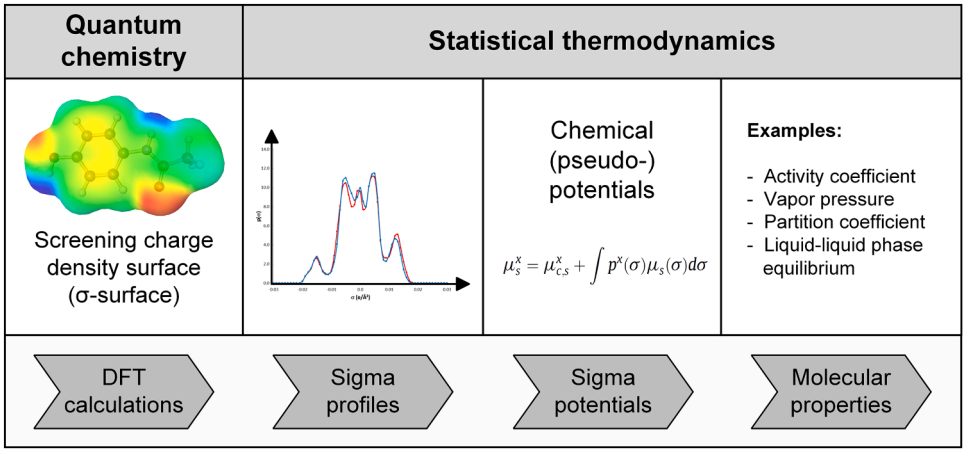

Fig. 2. Schematic representation of the COSMO-RS approach using quantum chemistry (density functional theory (DFT)) and statistical thermodynamics (sigma profiles and potentials) to obtain molecular properties. Further details about this schematic COSMO-RS approach can be inferred from the literature (Klamt, 2005; Klamt et al., 1998; Loschen and Klamt, 2012).

Table 2
Glass forming ability (GFA), the equilibrium solubility in the dissolution medium (phosphate buffer pH 6.8 with 0.5 % (w/v) DOSS), and the physiological charge state.

Substance	GFA class	Solubility [μg/mL]	Physiological charge state[F]
Carvedilol	III[A, B]	36.1 ± 0.01	+
Diclofenac (free acid)	III[B]	485.6 ± 0.00	−
Indomethacin	III[B, C, E]	485.1 ± 0.02	−
Ivermectin	III[B]	4.8 ± 0.01	0
Ketoconazole	III[A, B, C, E]	241.9 ± 0.02	0
Lopinavir	III[B, D]	34.4 ± 0.03	0
Pimozide	II[B]	113.9 ± 0.02	+
Probucol	III[A, B, E]	166.7 ± 0.02	0
Quinidine	II[B]	1013.2 ± 0.13	+
Ritonavir	III[A, B, D, E]	5.7 ± 0.02	0

Sources: A: (Alhalaweh et al., 2014); B: measured 2 heating & 2 cooling cycles (individually within a range of 25 °C - 270 °C and 10 °C/min) with DSC; C: (Panini et al., 2019); D: (Wyttenbach and Kuentz, 2017); E: (Baird et al., 2010); F: (Knox et al., 2024).

hypothesis for the current study, and 10 different drug-loaded mesoporous silica formulations were prepared via the incipient wetness impregnation method. To study drug desorption from silica surfaces, the drug-loading concentration was kept intentionally at the theoretical monolayer capacity level (MLC level), and the mass gain during the drug-loading process was gravimetrically verified to be close to the targeted MLC values (Table 1). Additionally, Table 2 shows the glass forming ability classification (class *I* = crystallize rapidly from a melt, II = crystallize slowly from a melt and III that do not crystallize from a melt upon re-heating and re-cooling (Baird et al., 2010)), the drug-solubility in the dissolution medium and the charge state at physiological conditions (+ = positively charged, - = negatively charged and 0 = neutral).

X-ray diffraction (XRD) and differential scanning calorimetry (DSC) were used for the basic drug state characterization. As a result, all formulation samples were predominantly amorphous. Possible traces of crystallinity can occur during the loading process, but this was not deemed as critical for formulation performance attributes as long as no further drug crystallization occurs. In addition to drug concentration, the pore size distribution of the mesoporous carrier material, glass-forming ability (GFA) of the drug, and choice of solvent during drug loading can significantly influence the success of amorphous drug loading. The GFA describes how readily a compound can form and remain in the amorphous (glassy) state, which is a key factor in designing amorphous solid dispersions (ASDs) (Augustijns and Brewster, 2012; Wyttenbach and Kuentz, 2017). Good glass formers (GFA class III) remain amorphous on cooling and reheating, while intermediate glass formers (GFA class II) form an amorphous glass but recrystallize over time during storage or upon reheating. Finally, poor glass formers (GFA class I) typically crystallize immediately upon cooling from a melt. It has been described that class II and I drugs can recrystallize during the solvent-based loading process, thereby blocking the mesopores of the carrier so that the drug possibly remains at the surface (Alhalaweh et al., 2014; Ditzinger et al., 2019; Wyttenbach and Kuentz, 2017). The GFA of the drugs used is shown in Table 2. For diclofenac (free acid), ivermectin, and quinidine, there was no information about the GFA available in the literature; therefore, the categorization was based on our own DSC measurements of the pure drug substance. Pimozide and quinidine exhibited a crystallization and a melting peak during the second heating and were therefore classified as GFA class II substances (see Table 2). The choice of mostly GFA III and class II compounds was to avoid drug crystallization issues during drug loading as well as to enable a better comparison of release profiles, that are potentially less complicated by fast drug precipitation on release (Ditzinger et al., 2019).

3.2. Calculations of chemical potential-based silica-water partitioning coefficient

To evaluate the partitioning behavior of selected APIs between a silica surface and an aqueous phase in silico (drug affinity to silica during dissolution), the chemical potentials in both environments were computed using COSMOquick, and the results are listed in Table 3.

The chemical potential for the self-association of drug molecules ($\mu s_{(self)}$) contributes to solubility but not explicitly to drug partitioning. Moreover, at a theoretical monolayer capacity (MLC), drug interactions with the silica surface are of higher importance than self-interactions of drug molecules, at least in diluted aqueous conditions. The last column in Table 3 gives the calculated silica-water partitioning coefficient in line with Eq. (3), and notable differences between the compounds were obtained. Higher values in this column suggest a relatively greater apparent drug affinity for silica in the presence of water. However, these calculations involve certain simplifications. Most notably, silica is assumed to be a supercooled bulk phase. Therefore, the current study aimed to derive a parameter capable of at least qualitatively ranking different drugs based on their affinity to silica during the drug release process.

Table 3
Calculated chemical (pseudo-) potentials for self-association ($\mu s_{(self)}$) and solvation (μs) between drug-silica, drug-water, and the silica-water partitioning coefficient of drug molecules ($\mu s_{(water)}$ - $\mu s_{(silica)}$) / RT (according to Eq. (3)) at 37 °C.

Substance name	$\mu s_{(self)}$ (kJ/mol)	$\mu s_{(silica)}$ (kJ/mol)	$\mu s_{(water)}$ (kJ/mol)	($\mu s_{(water)}$ - $\mu s_{(silica)}$) / RT (-)
Carvedilol	−14.44	−51.50	25.70	29.94
Diclofenac (free acid)	−8.78	−33.31	19.84	20.61
Indomethacin	−11.19	−39.53	19.82	23.02
Ivermectin	−62.78	−131.15	−10.42	46.82
Ketoconazole	−22.26	−81.66	6.07	34.02
Lopinavir	−37.13	−83.29	13.63	37.59
Pimozide	−27.39	−68.13	17.56	33.23
Probucol	−43.81	−74.65	27.38	39.57
Quinidine	−12.07	−43.24	17.60	23.59
Ritonavir	−34.81	−108.53	5.58	44.25

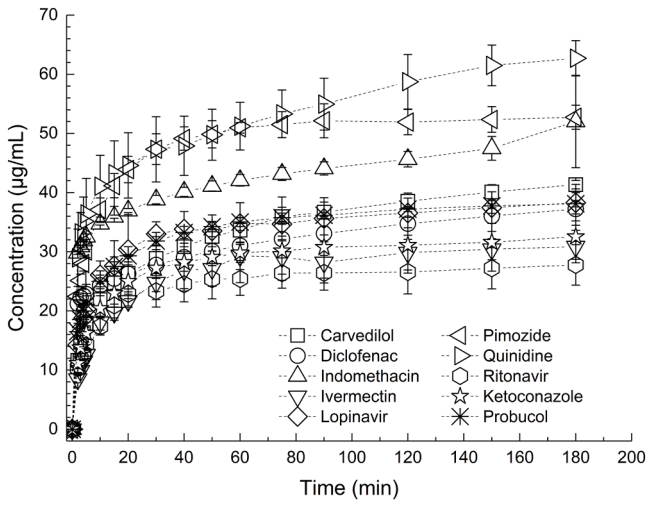

Fig. 3. Dissolution curves of 10 drug-loaded mesoporous silica formulations (n = 3) over 3 h at 37 °C in phosphate buffer (pH 6.8) and 0.5 % DOSS.

3.3. Experimental in vitro dissolution testing of drug-loaded silica formulations

Traditional dissolution testing is important for formulation development and characterization of bio-enabling drug delivery systems, like for example, supersaturating mesoporous silica-based formulations. It is important to consider that the design and execution of the dissolution test can strongly influence the outcomes of the study (Augustijns and Brewster, 2012). In this study, dissolution testing was performed using a USP Apparatus II (paddle method) with 250 mL of phosphate buffer (pH 6.8) containing 0.5 % (w/v) dioctyl sodium sulfosuccinate (DOSS) as the dissolution medium. All experiments were conducted at 37 ± 0.5 °C. Fig. 3 shows the course of the cumulative concentrations of the 10 pharmaceutical drugs. In all cases, drug dissolution from the mesoporous silica formulations was incomplete after 3 h of observation, which aligns with strong drug-silica interactions and potential re-adsorption processes, rather than late precipitation, as indicated by the stability of plateau concentrations throughout the observation period. The experimental design — incorporating monolayer drug loading to minimize drug-drug effects and a medium volume (250 mL) that transitioned from sink to non-sink conditions depending on solubility — was thus well-suited for investigating drug-silica interactions under controlled conditions. Among all tested APIs, quinidine exhibited the highest drug release after 3 h, with a release fraction of approximately 62 %. This, at physiological conditions positively charged drug substance, also showed the highest solubility in the dissolution media (see Table 2). In contrast, ketoconazole, ritonavir, and ivermectin demonstrated the lowest drug release over the same period, with a released fraction of approximately 22 %, 27 %, and 29 %, respectively. Ritonavir and ivermectin also possessed the lowest solubility in the dissolution media (Table 2). Notably, within the first two minutes of the dissolution process, at least 7 % of the drug was released across all formulations. The most pronounced increase in drug release occurred within the initial 5–10 min for all tested substances. Subsequently, the cumulative drug release rate slowed down considerably. After 90 min, a plateau for most drugs was reached, after which the drug concentration in the dissolution medium remained constant. Only carvedilol, diclofenac (free acid), indomethacin, and quinidine showed, in comparison to the beginning, a slower but continuous increase in drug dissolution till the end.

Theoretically, the steepness of the initial release slope would be to some extent determined by the drug-silica interactions. However, further molecular properties can be influential for drug release, so a high spring effect can, for example, affect the initial increase of drug concentrations (Sun and Lee, 2013). As for such a spring effect and hence the propensity of a drug to supersaturate, it was shown previously to greatly depend on GFA (Blaabjerg et al., 2018). As the model drugs in the current study were mostly good glass-forming compounds (Table 2), the effect of supersaturation propensity was not expected to dominate the overall drug release. However, it is still expected that such drug-specific properties beyond apparent drug affinity to silica would affect the kinetics of drug release from mesoporous formulations.

Table 4
Performance parameters of drug release kinetics (i.e., initial slopes and AUC values of drug concentrations 0–180 min) and supersaturation ratio at the end of the dissolution process (means of the last three points) of 10 drug-loaded mesoporous silica formulations (n = 3) at 37 °C.

Substance name	Initial slope of drug release [µg·mL^{-1}·min^{-1}]	AUC of concentrations [µg·min·mL^{-1}]	Supersaturation ratio[1] at the end of the experiment (180 min) [-]
Carvedilol	2.16 ± 0.09	6209± 349	1.11 ± 0.04
Diclofenac (free acid)	0.35 ± 0.05	5735± 434	0.074 ± 0.00
Indomethacin	1.02 ± 0.01	7745 ± 291	0.10 ± 0.00
Ivermectin	1.16 ± 0.12	4911 ± 374	6.33 ± 0.11
Ketoconazole	1.85 ± 0.15	5220 ± 829	0.13 ± 0.00
Lopinavir	1.67 ± 0.12	6154 ± 514	1.09 ± 0.03
Pimozide	1.77 ± 0.17	8840 ± 370	0.46 ± 0.00
Probucol	1.53 ± 0.11	6195 ± 134	0.23 ± 0.00
Quinidine	2.86 ± 0.15	9622 ± 746	0.06 ± 0.00
Ritonavir	1.42 ± 0.18	4506 ± 525	4.77 ± 0.11

1: Supersaturation ratio: (C/C_{sat}, where C is the drug concentration and C_{sat} is the equilibrium solubility).

Based on Fig. 3, the performance parameters (initial slopes and AUC values) were obtained. The supersaturation ratio was determined from the solubility-normalized concentrations at the end of the dissolution process, averaged from the last three measuring points of the plateau. Table 4 lists the results obtained for the three parameters for the selected 10 active pharmaceutical drugs (APIs). These calculated ratios indicate the final saturation level, where values < 1 represent undersaturated solutions, values equal to or close to 1 represent saturated solutions, and values > 1 represent supersaturated solutions.

Overall, ivermectin, ritonavir, carvedilol, and lopinavir showed the highest supersaturation levels at the end of the dissolution experiments, as reflected by the plateau region at the end of their respective dissolution curves. The fastest initial dissolution, as indicated by the slope values within the first 5–10 min, was observed for quinidine, carvedilol, and ketoconazole.

Remarkably, ivermectin and ritonavir were supersaturated during the entire dissolution experiment, while having the lowest solubility values in the dissolution media compared to the other drug substances (Tables 2 and 4). Carvedilol and lopinavir showed levels of a saturated solution state, whereas the rest of the drugs (diclofenac (free acid), indomethacin, ketoconazole, pimozide, probucol, and quinidine) were undersaturated during release kinetics (see Table 4). Moreover, quinidine, carvedilol, and ketoconazole exhibited the fastest initial dissolution rates, whereas quinidine, pimozide, and indomethacin demonstrated the highest area under the curve (AUC) values after 3 h. The results indicate that differences in relative saturation levels may contribute to a potential mechanism that can be confounded with apparent drug-carrier interactions, ultimately influencing drug release kinetics. However, from a practical perspective, it is common for more than one mechanism to govern the performance of a supersaturating formulation, either in vitro or in vivo (O'Dwyer et al., 2019).

3.4. Correlation analysis – chemical potentials as a predictive tool for qualitative dissolution performance?

As mentioned before, the calculated silica-water partitioning

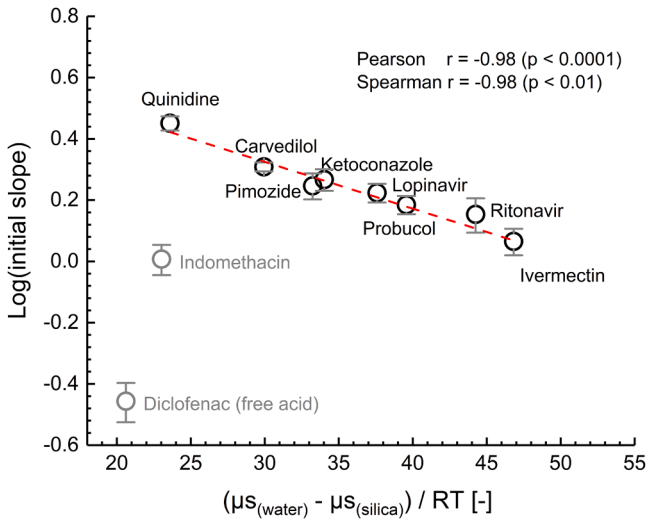

Fig. 4. Initial slope of drug release versus silica-water partition coefficient plot for eight drugs (and two outliers) with correlation coefficients. By definition, the slope was initially expressed in the following unit: [μg·mL^{-1}·min^{-1}].

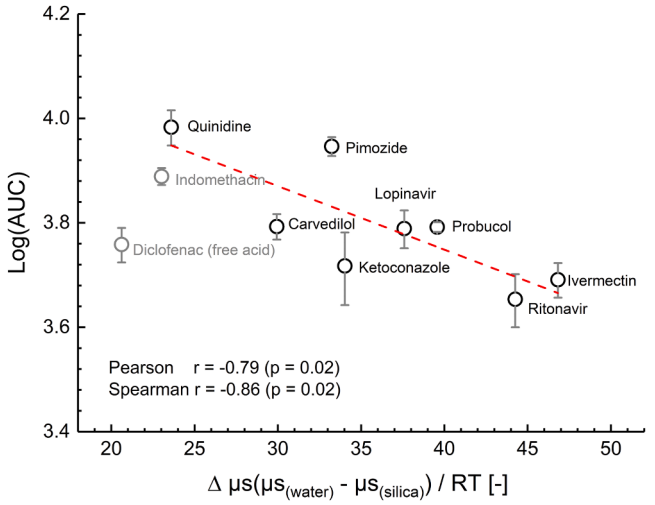

Fig. 5. Area under the curve (AUC) values versus silica-water partition coefficient plot for eight drugs with correlation coefficients. The AUC values were initially expressed in the following unit: [(μg·min)·mL^{-1}].

coefficient was coined as a potential characteristic of apparent drug-silica affinity to correlate with experimentally determined dissolution performance. A simplifying assumption here was treating silica as a supercooled bulk liquid. A similar assumption has been previously made, particularly when considering the solubility parameters of drugs in various solvation and solubility-related studies (Alanazi et al., 2020; Alqarni et al., 2021; Kalam et al., 2019; Shakeel et al., 2020; Shakeel and Alshehri, 2020). COSMO-RS is here certainly a more advanced way to model thermodynamic properties of drugs and their excipient mixtures, and it addresses several of the shortcomings of solubility parameters that were discussed before in the literature (Jankovic et al., 2019).

The silica-water partition coefficient, according to Eq. (3), was compared with the drug release characteristics. Thus, Figs. 4 and 5 display the linear shared correlations in scatter plots between the initial logarithmic slope or the area under the curve values (AUC until 180 min) on the y-axis and the silica-water partitioning coefficient (($\mu s_{(water)}$ - $\mu s_{(silica)}$) / RT) of the drugs on the x-axis. For the correlation analysis, only eight drugs were considered, while diclofenac (free acid) and indomethacin were treated as outliers. These two pharmaceutical active ingredients (APIs) belong to the group of nonsteroidal anti-inflammatory, small acidic drugs. Both have carboxyl groups and exist with pKa values of 4.0 and 4.5, mostly in a deprotonated/ionized form at physiological pH. Both showed a very low apparent affinity for silica (low silica-water partitioning coefficient), and except for quinidine, which had an even higher solubility, these two drugs showed the highest solubility in the phosphate buffer at pH 6.8. The relatively high solubility combined with the low carrier affinity was likely a key factor in the latter affinity not being prominently observed in the correlation analysis of the release performance of the two drugs. Besides exhibiting unusual studentized residuals (with values < 3) in the regression model, diclofenac is known to self-associate in aqueous media; the acid function interacts with itself and forms dimers (Kozlowska et al., 2018). It contains two aromatic rings and a chlorine-substituted, hydrophobic core. The carboxylate group makes it anionic, but the rest of the molecule is strongly hydrophobic, which promotes aggregation. Owing to this aggregation, the drug desorption kinetics (initial slope of drug concentration) were apparently reduced. Likewise, indomethacin is known to undergo self-association through the formation of hydrogen-bonded carboxylic acid dimers in solution (Taylor and Zografi, 1997), which can attenuate its apparent dissolution behavior. Therefore, the observed unusual studentized residuals of diclofenac and indomethacin in the regression analysis were attributed primarily to such self-aggregation.

Moreover, ionizable drug acids that exhibit relatively high solubility at an intestinal pH would not make best candidates for bio-enabling formulations, such as mesoporous silica-based drug delivery systems (Amidon et al., 1995; Charalabidis et al., 2019). The same arguments hold true for quinidine, which is classified as biopharmaceutical classification system (BCS) class I drug (Mori et al., 2012), whereas the other model compounds were drugs of class II (Buscarini et al., 2024; Chuasuwan et al., 2009; Fu et al., 2019; Guo et al., 2014; Hamed et al., 2016; Sodeifian et al., 2021; Steenekamp et al., 2024) and IV (Saeed et al., 2021; Salim et al., 2023). Overall, regarding the correlation analysis, the logarithmic initial slope values exhibited a strong linear Pearson correlation with the silica-water partitioning coefficient ($r = -0.98$, $p < 0.0001$) and a Spearman rank correlation of $r = -0.98$ ($p < 0.01$). The logarithmic AUC values also correlated with the silica-water partitioning coefficient, with a Pearson correlation of $r = -0.79$ ($p = 0.02$) and a Spearman rank correlation of $r = -0.86$ ($p = 0.02$). Additionally, when the logarithmic initial slope of the percentage of nominal drug released was considered, a Pearson correlation of $r = -0.86$ ($p = 0.006$) and a Spearman rank correlation of $r = 0.81$ ($p = 0.03$) with the silica-water partitioning coefficient were observed. These strong correlation relationships, illustrated in Figs. 4 and 5, indicate that a higher silica-water partitioning coefficient reflects a greater affinity of the drug to the silica surface and, consequently, a lower initial slope of drug release into the dissolution medium.

Similarly, Fig. 5 illustrates that a greater affinity to silica corresponds to a lower area under the curve (AUC) of the dissolved drug concentrations over the entire dissolution period (180 min). However, as indomethacin and diclofenac (free acid) were the only negatively charged drugs (Table 2), their release kinetics were not expected to depend significantly on silica interaction under ionizing pH conditions, as mentioned previously. Ionizable acids are expected to weakly interact with silica because of repulsive forces. However, as discussed earlier, drug aggregation via the carboxylate groups could have greatly reduced such repulsive forces in the experiments. As the *in silico* model was not taking such aggregates into account, this would explain the deviation from the general trendline. The topic of electrostatic interactions is of broader interest. In this regard, previous work (Hate et al., 2020a) investigated the effects of electrostatic interactions between drug molecules and silica surface on the dissolution of weakly basic drugs from mesoporous silica-based formulations as a function of medium pH. The authors concluded from their findings that, compared to the formation of hydrogen bonding interactions, drug-silica electrostatic interactions lead to higher adsorption and lower drug release. The experimental data

in the present work supports such a view, that strong interactions with silica limit drug release, but also suggests that electrostatic interactions alone do not fully account for the observed desorption behavior. For example, carvedilol, a weak base with a pKa of approximately 7.8 is primarily protonated and thus positively charged at pH 6.8 (Yuvaraja and Khanam, 2014). Although this leads to attractive electrostatic interactions between the drug and the negatively charged silica surface, carvedilol showed a relatively low silica water partitioning coefficient and therefore limited drug-silica affinity (Figs. 4 and 5). The complexity of the dissolution process of a drug-loaded mesoporous silica formulation can be largely attributed to the interplay of more than one contributing factor; therefore, the release kinetics of any compound are not governed solely by the charge state of the drug at the pH of the dissolution medium.

In Fig. 5, the previously identified "outliers" for the initial slope of drug concentrations, diclofenac (free acid) and indomethacin, are less distant from the data cloud of the other drugs. They were not included in the correlation analysis for consistency and hence, comparability of the analysis in Fig. 4. While this previous analysis focused on the initial stage of the drug release process, the AUC values are representative of the drug dissolution process over the entire experimental time (3 h). During this long dissolution time, other influential factors besides drug desorption from silica can be influential regarding the dissolution performance. In general, it is expected that the physicochemical properties that govern solubility and supersaturation propensity influence kinetic profiles and have a higher impact on the AUC of the entire experiment duration compared to the short time of the initial release. However, according to the dissolution profiles in Fig. 3, the drug concentration plateaus were not all leveling off during the 3 h observation time. There were no decreases in concentrations observed that could have otherwise indicated a marked drug precipitation of drugs that were supersaturated.

Notably, quinidine exhibited extreme behavior across several drug properties, including the highest solubility in the dissolution medium (lowest supersaturation ratio), highest initial drug release and AUC plateau values, and low affinity to silica. In contrast, ivermectin had the lowest solubility in the dissolution medium (highest supersaturation ratio), a medium initial slope of drug concentration, low AUC level, and highest affinity to silica. In summary, the release process from mesoporous silica appears to be governed by a complex interplay of multiple factors; however, the apparent drug-silica affinity plays a dominant role, especially in the initial stage of drug release. Overall, it is very encouraging that, for neutral and positively charged drugs, there was a very good correlation found between the silica-water partitioning coefficient (based on chemical potentials) and the experimental performance parameters of drug release (initial slopes and AUC values). Still, despite extended observation over 3 h, none of the tested active pharmaceutical ingredients (APIs) achieved complete release, suggesting that a fraction of drug molecules remained adsorbed to the mesoporous silica surface. This persistent retention likely reflects a dynamic equilibrium between desorption and re-adsorption processes, as previously observed in the literature (Turku et al., 2007). Another study (McCarthy et al., 2018) further showed that the extent of irreversible adsorption is highly pH-dependent. Given the isoelectric point of silica (~pH 2), its surface bears a significant negative charge at physiological and higher pH levels, with charge density increasing markedly between pH 6 and 11 (Atkin et al., 2003; Sharma et al., 1996), and this promotes in particular electrostatic interactions.

Incomplete release from mesoporous systems is a widely reported phenomenon, even at low drug loadings (Le et al., 2019), and is commonly attributed to reversible and irreversible drug-silica interactions (Hate et al., 2020a). Consistent with this, the literature describes cases of incomplete release for most evaluated drugs in this study (i.e., ritonavir and lopinavir (Dening et al., 2019), indomethacin (Garcia-Bennett et al., 2018; McCarthy et al., 2020), ketoconazole (Hate et al., 2020a), ivermectin (Velho et al., 2024), carvedilol (Mahdi et al., 2022), diclofenac (Ghiorghita et al., 2022), probucol (Lau et al., 2019)). If sink conditions or a diffusion barrier (membrane) are present, release may approach completion better, as there would be a sink for the drug to diffuse away. Hate et al. (Hate et al., 2020a) e.g., showed that atazanavir eventually reached 100 % release when an absorptive sink was used.

The utility of COSMO-RS chemical potentials to approximate the silica-water partitioning behavior, and their strong correlation with drug release metrics (i.e., initial slope and AUC), provides the means to at least rank formulation release performance. This is encouraging for formulation scientists, who can harness this approach for formulation development.

In the future, more experiments with different drug candidates, higher drug loadings, and different aqueous surrounding dissolution media should be performed for a more complete understanding of the molecular drug-silica interactions during the complex release process.

4. Conclusions

This study introduces a novel *in silico* method for investigating drug-silica interactions in aqueous environments, addressing a critical knowledge gap in the rational design of mesoporous silica-based delivery systems for poorly soluble drugs. Using a silica-water drug partitioning coefficient from COSMO-RS calculations, good linear and rank correlations with the experimental drug release characteristics were obtained. The findings of this study underscore the importance of considering drug-specific physicochemical properties, such as ionization state, solubility, and glass-forming ability, in tandem with the surface characteristics of the mesoporous silica carrier (surface area, pore size, and silanol-siloxane ratio). Notably, while electrostatic interactions contribute substantially to the drug affinity for the silica surface, they do not solely govern the desorption process. The results support the view that drug release kinetics from mesoporous silica systems are not dictated by a single dominant interaction but rather by the collective effect of multiple, often competing, molecular mechanisms.

The current study compared drugs relative to their ability to form a monolayer on the carrier surface. At such low drug loadings near the theoretical monolayer capacity (MLC), the dominant interactions occur at the solid-liquid interface and involve a complex balance of electrostatic attraction or repulsion (Hate et al., 2020a, 2020b), hydrogen bonding, and dispersion (van der Waals) forces, suggesting a persistent equilibrium between desorption and re-adsorption, and highlighting the potential for irreversible binding phenomena (McCarthy et al., 2018, 2016). The presented *in silico* approach offered a valuable theory-based tool to at least qualitatively rank drug release performance. This would be highly valuable in a pharmaceutical profiling phase where minimal amounts of drug are available to guide formulation development. By enabling an early mechanism-based ranking of drug-silica interactions, this method also has the potential to reduce the experimental screening time in preformulation practice.

While this study focused on GFA class III drugs with low drug loading to enable a clear mechanistic interpretation of silica-water partitioning effects, future investigations may extend this approach to include GFA class I compounds. However, due to their poor amorphous stability and high crystallization tendency, such compounds would require specifically adapted formulation strategies, such as surface functionalization of the carrier or co-formulation with crystallization inhibitors. In a broader context, future work should also explore different drug loadings and dissolution media at varying pH values to gain further insight into how these factors influence drug-silica interactions and ultimately drug release. Moreover, the development of quantitative models for drug release may benefit from incorporating additional physicochemical parameters of the carrier material. However, the present study already contributes to advancing the mechanistic understanding of apparent drug-silica interactions, thereby supporting the rational design of mesoporous silica-based drug delivery systems.

CRediT authorship contribution statement

Andreas Niederquell: Writing – original draft, Visualization, Methodology, Investigation, Formal analysis, Data curation, Conceptualization. **Annika Hofer:** Investigation, Formal analysis. **Barbora Vraníková:** Writing – review & editing, Supervision, Resources, Conceptualization. **Martin Kuentz:** Writing – review & editing, Supervision, Resources, Conceptualization.

Declaration of competing interest

The authors declare that they have no known competing financial interests or personal relationships that could have appeared to influence the work reported in this paper.

Acknowledgements

This study was supported by Charles University (SVV 260 661), Charles University Grant Agency (Grant No 337622/2022), and the project New Technologies for Translational Research in Pharmaceutical Sciences/NETPHARM, ID CZ.02.01.01/00/22_008/0004607, co-funded by the European Union.

Data availability

Data will be made available on request.

References

Alanazi, A., Alshehri, S., Altamimi, M., Shakeel, F., 2020. Solubility determination and three dimensional Hansen solubility parameters of gefitinib in different organic solvents: experimental and computational approaches. J. Mol. Liq. 299. https://doi.org/10.1016/j.molliq.2019.112211.

Alhalaweh, A., Alzghoul, A., Kaialy, W., Mahlin, D., Bergström, C.A.S., 2014. Computational predictions of glass-forming ability and crystallization tendency of drug molecules. Mol. Pharm. 11, 3123–3132. https://doi.org/10.1021/mp500303a.

Alqarni, M.H., Haq, N., Alam, P., Abdel-Kader, M.S., Foudah, A.I., Shakeel, F., 2021. Solubility data, Hansen solubility parameters and thermodynamic behavior of pterostilbene in some pure solvents and different (PEG-400 + water) cosolvent compositions. J. Mol. Liq. 331. https://doi.org/10.1016/j.molliq.2021.115700.

Amidon, G.L., Lennernäs, H., Shah, V.P., Crison, J.R., 1995. A theoretical basis for a biopharmaceutic drug classification: the correlation of in vitro drug product dissolution and in vivo bioavailability. Pharm. Res. 12, 413–420.

Argyo, C., Weiss, V., Bräuchle, C., Bein, T., 2014. Multifunctional mesoporous silica nanoparticles as a universal platform for drug delivery. Chem. Mater. https://doi.org/10.1021/cm402592t.

Atkin, R., Craig, V.S.J., Wanless, E.J., Biggs, S., 2003. Mechanism of cationic surfactant adsorption at the solid-aqueous interface. Adv. Colloid. Interface Sci. https://doi.org/10.1016/S0001-8686(03)00002-2.

Augustijns, P., Brewster, M.E., 2012. Supersaturating drug delivery systems: fast is not necessarily good enough. J. Pharm. Sci. https://doi.org/10.1002/jps.22750.

Baird, J.A., Van Eerdenbrugh, B., Taylor, L.S., 2010. A classification system to assess the crystallization tendency of organic molecules from undercooled melts. J. Pharm. Sci. 99, 3787–3806. https://doi.org/10.1002/jps.22197.

Bavnhøj, C.G., Knopp, M.M., Madsen, C.M., Löbmann, K., 2019. The role interplay between mesoporous silica pore volume and surface area and their effect on drug loading capacity. Int. J. Pharm. X. 1. https://doi.org/10.1016/j.ijpx.2019.100008.

Blaabjerg, L.I., Lindenberg, E., Löbmann, K., Grohganz, H., Rades, T., 2018. Is there a correlation between the glass forming ability of a drug and its supersaturation propensity? Int. J. Pharm. 538, 243–249. https://doi.org/10.1016/j.ijpharm.2018.01.013.

Bremmell, K.E., Prestidge, C.A., 2019. Enhancing oral bioavailability of poorly soluble drugs with mesoporous silica based systems: opportunities and challenges. Drug Dev. Ind. Pharm. https://doi.org/10.1080/03639045.2018.1542709.

Buscarini, A., Zaworotko, M.J., Matos, C.R.M.O., Grepioni, F., Contini, L., Capsoni, D., Friuli, V., Maggi, L., Bruni, G., 2024. Pimozide and Adipic acid: a new multicomponent crystalline entity for improved pharmaceutical behavior. Molecules. 29. https://doi.org/10.3390/molecules29235610.

Charalabidis, A., Sfouni, M., Bergström, C., Macheras, P., 2019. The Biopharmaceutics Classification System (BCS) and the Biopharmaceutics Drug Disposition Classification System (BDDCS): beyond guidelines. Int. J. Pharm. https://doi.org/10.1016/j.ijpharm.2019.05.041.

Chiou, W.L., Keyphrases, S.R., 1971. Pharmaceutical applications of Solid dispersion systems 60. doi:10.1002/jps.2600600902.

Chuasuwan, B., Binjesoh, V., Polli, J.E., Zhang, H., Amidon, G.L., Junginger, H.E., Midha, K.K., Shah, V.P., Stavchansky, S., Dressman, J.B., Barends, D.M., 2009. Biowaiver monographs for immediate release solid oral dosage forms: diclofenac sodium and diclofenac potassium. J. Pharm. Sci. https://doi.org/10.1002/jps.21525.

Delle Piane, M., Corno, M., Pedone, A., Dovesi, R., Ugliengo, P., 2014. Large-scale B3LYP simulations of ibuprofen adsorbed in MCM-41 mesoporous silica as drug delivery system. J. Phys. Chem. C 118, 26737–26749. https://doi.org/10.1021/jp507364h.

Dening, T.J., Taylor, L.S., 2018. Supersaturation potential of ordered mesoporous silica delivery systems. Part 1: dissolution performance and drug membrane transport rates. Mol. Pharm. 15, 3489–3501. https://doi.org/10.1021/acs.molpharmaceut.8b00488.

Dening, T.J., Zemlyanov, D., Taylor, L.S., 2019. Application of an adsorption isotherm to explain incomplete drug release from ordered mesoporous silica materials under supersaturating conditions. J. Control. Release 307, 186–199. https://doi.org/10.1016/j.jconrel.2019.06.028.

Ditzinger, F., Price, D.J., Nair, A., Becker-Baldus, J., Glaubitz, C., Dressman, J.B., Saal, C., Kuentz, M., 2019. Opportunities for successful stabilization of poor glass-forming drugs: a stability-based comparison of mesoporous silica versus hot melt extrusion technologies. Pharmaceutics 11. https://doi.org/10.3390/pharmaceutics11110577.

Eckert, F., Klamt, A., 2002. Fast solvent screening via Quantum chemistry: COSMO-RS approach. AIChE J. 48, 369–385. https://doi.org/10.1002/aic.690480220.

Eugene Papirer, 2000. Adsorption on silica surfaces. doi:10.1201/9781482269703.

Fu, Q., Lu, H.D., Xie, Y.F., Liu, J.Y., Han, Y., Gong, N.B., Guo, F., 2019. Salt formation of two BCS II drugs (indomethacin and naproxen) with (1R, 2R)-1,2-diphenylethylenediamine: crystal structures, solubility and thermodynamics analysis. J. Mol. Struct. 1185, 281–289. https://doi.org/10.1016/j.molstruc.2019.02.104.

Garcia-Bennett, A.E., Lau, M., Bedford, N., 2018. Probing the amorphous State of pharmaceutical compounds within mesoporous material using pair distribution function analysis. J. Pharm. Sci. 107, 2216–2224. https://doi.org/10.1016/j.xphs.2018.03.029.

Ghiorghita, C.A., Dinu, M.V., Dragan, E.S., 2022. Burst-free and sustained release of diclofenac sodium from mesoporous silica/PEI microspheres coated with carboxymethyl cellulose/chitosan layer-by-layer films. Cellulose 29, 395–412. https://doi.org/10.1007/s10570-021-04282-y.

Gignone, A., Delle Piane, M., Corno, M., Ugliengo, P., Onida, B., 2015. Simulation and experiment reveal a complex scenario for the adsorption of an antifungal drug in ordered mesoporous silica. J. Phys. Chem. C 119, 13068–13079. https://doi.org/10.1021/acs.jpcc.5b02666.

Guo, B., Liu, H., Li, Y., Zhao, J., Yang, D., Wang, X., Zhang, T., 2014. Application of phospholipid complex technique to improve the dissolution and pharmacokinetic of probucol by solvent-evaporation and co-grinding methods. Int. J. Pharm. 474, 50–56. https://doi.org/10.1016/j.ijpharm.2014.08.006.

Hamed, R., Awadallah, A., Sunoqrot, S., Tarawneh, O., Nazzal, S., AlBaraghthi, T., Al Sayyad, J., Abbas, A., 2016. pH-dependent solubility and dissolution behavior of Carvedilol—Case example of a weakly basic BCS class II drug. AAPS. PharmSciTech. 17, 418–426. https://doi.org/10.1208/s12249-015-0365-2.

Hate, S.S., Reutzel-Edens, S.M., Taylor, L.S., 2020a. Influence of drug-silica electrostatic interactions on drug release from mesoporous silica-based oral delivery systems. Mol. Pharm. 17, 3435–3446. https://doi.org/10.1021/acs.molpharmaceut.0c00488.

Hate, S.S., Reutzel-Edens, S.M., Taylor, L.S., 2020b. Interplay of adsorption, supersaturation and the presence of an absorptive sink on drug release from mesoporous silica-based formulations. Pharm. Res. 37. https://doi.org/10.1007/s11095-020-02879-9.

Jankovic, S., Tsakiridou, G., Ditzinger, F., Koehl, N.J., Price, D.J., Ilie, A.R., Kalantzi, L., Kimpe, K., Holm, R., Nair, A., Griffin, B., Saal, C., Kuentz, M., 2019. Application of the solubility parameter concept to assist with oral delivery of poorly water-soluble drugs – a PEARRL review. J. Pharm. Pharmacol. https://doi.org/10.1111/jphp.12948.

Kalam, M.A., Alshehri, S., Alshamsan, A., Alkholief, M., Ali, R., Shakeel, F., 2019. Solubility measurement, Hansen solubility parameters and solution thermodynamics of gemfibrozil in different pharmaceutically used solvents. Drug Dev. Ind. Pharm. 45, 1258–1264. https://doi.org/10.1080/03639045.2019.1594884.

Kawabata, Y., Wada, K., Nakatani, M., Yamada, S., Onoue, S., 2011. Formulation design for poorly water-soluble drugs based on biopharmaceutics classification system: basic approaches and practical applications. Int. J. Pharm. https://doi.org/10.1016/j.ijpharm.2011.08.032.

Khalbas, A.H., Albayati, T.M., Ali, N.S., Salih, I.K., 2024a. Drug loading methods and kinetic release models using of mesoporous silica nanoparticles as a drug delivery system: a review. S. Afr. J. Chem. Eng. https://doi.org/10.1016/j.sajce.2024.08.013.

Khalbas, A.H., Albayati, T.M., Saady, N.M.C., Zendehboudi, S., Salih, I.K., Tofah, M.L., 2024b. Insights into drug loading techniques with mesoporous silica nanoparticles: optimization of operating conditions and assessment of drug stability. J. Drug Deliv. Sci. Technol. https://doi.org/10.1016/j.jddst.2024.105698.

Khan, K.U., Minhas, M.U., Badshah, S.F., Suhail, M., Ahmad, A., Ijaz, S., 2022. Overview of nanoparticulate strategies for solubility enhancement of poorly soluble drugs. Life Sci. https://doi.org/10.1016/j.lfs.2022.120301.

Klajmon, M., 2022. Purely predicting the pharmaceutical solubility: what to expect from PC-SAFT and COSMO-RS? Mol. Pharm. 19, 4212–4232. https://doi.org/10.1021/acs.molpharmaceut.2c00573.

Klamt, A., 2011. The COSMO and COSMO-RS solvation models. Wiley. Interdiscip. Rev. Comput. Mol. Sci. https://doi.org/10.1002/wcms.56.

Klamt, A., 2005. COSMO-RS From Quantum Chemistry to Fluid Phase Thermodynamics and Drug Design, 1st ed. Elsevier, Leverkusen.

Klamt, A., 1995. Conductor-like screening model for real solvents: a new approach to the quantitative calculation of solvation phenomena. J. Phys. Chem.

Klamt, A., Eckert, F., Hornig, M., Beck, M.E., Brger, T., 2002. Prediction of aqueous solubility of drugs and pesticides with COSMO-RS. J. Comput. Chem. 23, 275–281. https://doi.org/10.1002/jcc.1168.

Klamt, A., Jonas, V., Bu, T., Lohrenz, J.C.W., 1998. Refinement and parametrization of COSMO-RS.

Knox, C., Wilson, M., Klinger, C.M., Franklin, M., Oler, E., Wilson, A., Pon, A., Cox, J., Chin, N.E.L., Strawbridge, S.A., Garcia-Patino, M., Kruger, R., Sivakumaran, A., Sanford, S., Doshi, R., Khetarpal, N., Fatokun, O., Doucet, D., Zubkowski, A., Rayat, D.Y., Jackson, H., Harford, K., Anjum, A., Zakir, M., Wang, F., Tian, S., Lee, B., Liigand, J., Peters, H., Wang, R.Q.R., Nguyen, T., So, D., Sharp, M., da Silva, R., Gabriel, C., Scantlebury, J., Jasinski, M., Ackerman, D., Jewison, T., Sajed, T., Gautam, V., Wishart, D.S., 2024. DrugBank 6.0: the DrugBank Knowledgebase for 2024 [WWW Document]. Nucleic. Acids. Res. https://doi.org/10.1093/nar/gkad976.

Kozlowska, M., Rodziewicz, P., Utesch, T., Mroginski, M.A., Kaczmarek-Kedziera, A., 2018. Solvation of diclofenac in water from atomistic molecular dynamics simulations-interplay between solute-solute and solute-solvent interactions. Phys. Chem. Chem. Phys. 20, 8629–8639. https://doi.org/10.1039/c7cp08468d.

Lau, M., Giri, K., Garcia-Bennett, A.E., 2019. Antioxidant properties of probucol released from mesoporous silica. Eur. J. Pharm. Sci. 138. https://doi.org/10.1016/j.ejps.2019.105038.

Le, T.T., Elyafi, A.K.E., Mohammed, A.R., Al-Khattawi, A., 2019. Delivery of poorly soluble drugs via mesoporous silica: impact of drug overloading on release and thermal profiles. Pharmaceutics. 11. https://doi.org/10.3390/pharmaceutics11060269.

Leuner, C., Dressman, J., 2000. Improving drug solubility for oral delivery using solid dispersions 50. doi:10.1016/S0939-6411(00)00076-X.

Loschen, C., Klamt, A., 2015. Solubility prediction, solvate and cocrystal screening as tools for rational crystal engineering. J. Pharm. Pharmacol. 67, 803–811. https://doi.org/10.1111/jphp.12376.

Loschen, C., Klamt, A., 2012. COSMO quick: a novel interface for fast σ-profile composition and its application to COSMO-RS solvent screening using multiple reference solvents. Ind. Eng. Chem. Res. 51, 14303–14308. https://doi.org/10.1021/ie3023675.

Mac Fhionnlaoich, N., Zeglinski, J., Simon, M., Wood, B., Davin, S., Glennon, B., 2024. A hybrid approach to aqueous solubility prediction using COSMO-RS and machine learning. Chem. Eng. Res. Des. 209, 67–71. https://doi.org/10.1016/j.cherd.2024.07.050.

Mahdi, H.S., Muhana, F.J.I., Al-Ani, I.H., Al-Sanabrah, A., 2022. Preparation and evaluation of SBA-16, ZSM-5 and MCM-41 mesoporous silica nanoparticles as drug delivery system for Carvedilol. Int. J. Drug Deliv. Technol. 12, 1033–1048. https://doi.org/10.25258/ijddt.12.3.20.

Mahmoudabadi, S.Z., Pazuki, G., 2020. Investigation of COSMO-SAC model for solubility and cocrystal formation of pharmaceutical compounds. Sci. Rep. 10. https://doi.org/10.1038/s41598-020-76986-3.

Maleki, A., Kettiger, H., Schoubben, A., Rosenholm, J.M., Ambrogi, V., Hamidi, M., 2017. Mesoporous silica materials: from physico-chemical properties to enhanced dissolution of poorly water-soluble drugs. J. Control. Release. https://doi.org/10.1016/j.jconrel.2017.07.047.

McCarthy, C.A., Ahern, R.J., Devine, K.J., Crean, A.M., 2018. Role of drug adsorption onto the silica surface in drug release from mesoporous silica systems. Mol. Pharm. 15, 141–149. https://doi.org/10.1021/acs.molpharmaceut.7b00778.

McCarthy, C.A., Ahern, R.J., Dontireddy, R., Ryan, K.B., Crean, A.M., 2016. Mesoporous silica formulation strategies for drug dissolution enhancement: a review. Expert. Opin. Drug Deliv. 13, 93–108. https://doi.org/10.1517/17425247.2016.1100165.

McCarthy, C.A., Zemlyanov, D.Y., Crean, A.M., Taylor, L.S., 2020. Comparison of drug release and adsorption under supersaturating conditions for ordered mesoporous silica with indomethacin or indomethacin methyl ester. Mol. Pharm. 17, 3062–3074. https://doi.org/10.1021/acs.molpharmaceut.0c00489.

Mehmood, A., Ghafar, H., Yaqoob, S., Gohar, U.F., Ahmad, B., 2017. Mesoporous silica nanoparticles: a review. J. Dev. Drugs 06. https://doi.org/10.4172/2329-6631.1000174.

Mori, N., Iwamoto, H., Yokooji, T., Murakami, T., 2012. Characterization of intestinal absorption of quinidine, a P-glycoprotein substrate, given as a powder in rats. Pharmazie 67, 384–388. https://doi.org/10.1691/ph.2012.1700.

Narayan, R., Gadag, S., Garg, S., Nayak, U.Y., 2022. Understanding the effect of functionalization on loading capacity and release of drug from mesoporous silica nanoparticles: a computationally driven study. ACS. Omega 7, 8229–8245. https://doi.org/10.1021/acsomega.1c03618.

Narayan, R., Nayak, U.Y., Raichur, A.M., Garg, S., 2018. Mesoporous silica nanoparticles: a comprehensive review on synthesis and recent advances. Pharmaceutics. https://doi.org/10.3390/pharmaceutics10030118.

Niederquell, A., Vraníková, B., Kuentz, M., 2023. Study of disordered mesoporous silica regarding intrinsic compound affinity to the carrier and drug-accessible surface area. Mol. Pharm. 20, 6301–6310. https://doi.org/10.1021/acs.molpharmaceut.3c00690.

Niederquell, A., Vraníková, B., Kuentz, M., 2025. Ranking of apparent drug affinity to mesoporous silica utilizing a chromatographic screening method and a tree-based prediction model. Int. J. Pharm. 682, 1–11. https://doi.org/10.1016/j.ijpharm.2025.125918.

O'Dwyer, P.J., Litou, C., Box, K.J., Dressman, J.B., Kostewicz, E.S., Kuentz, M., Reppas, C., 2019. In vitro methods to assess drug precipitation in the fasted small intestine – a PEARRL review. J. Pharm. Pharmacol. https://doi.org/10.1111/jphp.12951.

Panini, P., Rampazzo, M., Singh, A., Vanhoutte, F., Van den Mooter, G., 2019. Myth or truth: the glass forming ability class III drugs will always form single-phase homogenous amorphous solid dispersion formulations. Pharmaceutics 11. https://doi.org/10.3390/pharmaceutics11100529.

Prestidge, C.A., Barnes, T.J., Lau, C.H., Barnett, C., Loni, A., Canham, L., 2007. Mesoporous silicon: a platform for the delivery of therapeutics. Expert. Opin. Drug Deliv. https://doi.org/10.1517/17425247.4.2.101.

Qian, K.K., Bogner, R.H., 2012. Application of mesoporous silicon dioxide and silicate in oral amorphous drug delivery systems. J. Pharm. Sci. https://doi.org/10.1002/jps.22779.

Roggers, R., Kanvinde, S., Boonsith, S., Oupický, D., 2014. The practicality of mesoporous silica nanoparticles as drug delivery devices and progress toward this goal. AAPS. PharmSciTech. https://doi.org/10.1208/s12249-014-0142-7.

Saeed, A.M., Schmidt, J.M., Munasinghe, W.P., Vallabh, B.K., Jarvis, M.F., Morris, J.B., Mostafa, N.M., 2021. Comparative bioavailability of two formulations of biopharmaceutical classification system (BCS) class IV drugs: a case study of Lopinavir/Ritonavir. J. Pharm. Sci. 110, 3963–3968. https://doi.org/10.1016/j.xphs.2021.08.037.

Salim, M., Ramirez, G., Clulow, A.J., Hawley, A., Boyd, B.J., 2023. Implications of the digestion of milk-based formulations for the solubilization of Lopinavir/Ritonavir in a combination therapy. Mol. Pharm. 20, 2256–2265. https://doi.org/10.1021/acs.molpharmaceut.3c00072.

Santos, H., Salonen, J., Bimbo, L., Lehto, V., Peltonen, L., Hirvonen, J., 2011. Mesoporous materials as controlled drug delivery formulations.

Shakeel, F., Alshehri, S., 2020. Solubilization, hansen solubility parameters, solution thermodynamics and solvation behavior of flufenamic acid in (carbitol + water) mixtures. Processes 8. https://doi.org/10.3390/PR8101204.

Shakeel, F., Haq, N., Alsarra, I.A., Alshehri, S., 2020. Solubility, Hansen solubility parameters and thermodynamic behavior of emtricitabine in various (polyethylene glycol-400 + water) mixtures: computational modeling and thermodynamics. Molecules. 25. https://doi.org/10.3390/molecules25071559.

Sharma, R., Treiner, C., Monticone, V., 1996. In: Surfactant Adsorption and Surface Solubilization- ACS Symposium series 615. Washington, DC. American Chemical Society. https://doi.org/10.1021/bk-1995-0615.

Sodeifian, G., Sajadian, S.A., Razmimanesh, F., Hazaveie, S.M., 2021. Solubility of ketoconazole (antifungal drug) in SC-CO2 for binary and ternary systems: measurements and empirical correlations. Sci. Rep. 11. https://doi.org/10.1038/s41598-021-87243-6.

Steenekamp, E.M., Liebenberg, W., Lemmer, H.J.R., Gerber, M., 2024. Formulation and ex vivo evaluation of ivermectin within different nano-drug delivery vehicles for transdermal drug delivery. Pharmaceutics. 16, 1466. https://doi.org/10.3390/pharmaceutics16111466.

Sun, D.D., Lee, P.I., 2013. Evolution of supersaturation of amorphous pharmaceuticals: the effect of rate of supersaturation generation. Mol. Pharm. 10, 4330–4346. https://doi.org/10.1021/mp400439q.

Tang, F., Li, L., Chen, D., 2012. Mesoporous silica nanoparticles: synthesis, biocompatibility and drug delivery. Adv. Mater. 24, 1504–1534. https://doi.org/10.1002/adma.201104763.

Taylor, S.L., Zografi, G., 1997. Spectroscopic characterization of interactions between PVP and indomethacin in amorphous molecular dispersions. Pharm. Res. 14, 1691–1698. https://doi.org/10.1023/A:1012167410376.

Turku, I., Sainio, T., Paatero, E., 2007. Thermodynamics of tetracycline adsorption on silica. Environ. Chem Lett. 5, 225–228. https://doi.org/10.1007/s10311-007-0106-1.

Vallet-Regí, M., Colilla, M., Izquierdo-Barba, I., Manzano, M., 2018. Mesoporous silica nanoparticles for drug delivery: current insights. Molecules. https://doi.org/10.3390/molecules23010047.

Velho, M.C., Funk, N.L., Deon, M., Benvenutti, E.V., Buchner, S., Hinrichs, R., Pilger, D.A., Beck, R.C.R., 2024. Ivermectin-loaded mesoporous silica and polymeric nanocapsules: impact on drug loading, In vitro solubility enhancement, and release performance. Pharmaceutics 16. https://doi.org/10.3390/pharmaceutics16030325.

Vraníková, B., Niederquell, A., Šklubalová, Z., Kuentz, M., 2020. Relevance of the theoretical critical pore radius in mesoporous silica for fast crystallizing drugs. Int. J. Pharm. 591. https://doi.org/10.1016/j.ijpharm.2020.120019.

Warnau, J., Wichmann, K., Reinisch, J., 2021. COSMO-RS predictions of logP in the SAMPL7 blind challenge. J. Comput. Aided. Mol. Des. 35, 813–818. https://doi.org/10.1007/s10822-021-00395-5.

Wyttenbach, N., Kirchmeyer, W., Alsenz, J., Kuentz, M., 2016. Theoretical considerations of the prigogine-defay ratio with regard to the glass-forming ability of drugs from undercooled melts. Mol. Pharm. 13, 241–250. https://doi.org/10.1021/acs.molpharmaceut.5b00688.

Wyttenbach, N., Kuentz, M., 2017. Glass-forming ability of compounds in marketed amorphous drug products. Eur. J. Pharm. Biopharm. 112, 204–208. https://doi.org/10.1016/j.ejpb.2016.11.031.

Yuvaraja, K., Khanam, J., 2014. Enhancement of carvedilol solubility by solid dispersion technique using cyclodextrins, water soluble polymers and hydroxyl acid. J. Pharm. Biomed. Anal. 96, 10–20. https://doi.org/10.1016/j.jpba.2014.03.019.

Zhang, H., Li, M., Li, J., Agrawal, A., Hui, H.W., Liu, D., 2022. Superiority of mesoporous silica-based amorphous formulations over spray-dried solid dispersions. Pharmaceutics 14. https://doi.org/10.3390/pharmaceutics14020428.